Effect of Peripheral Convection on Tropical Cyclone Formation

MARJA BISTER

Meteorological Research, Finnish Meteorological Institute, Helsinki, Finland

(Manuscript received 24 May 2000, in final form 10 April 2001)

ABSTRACT

The effect of peripheral convection on the formation and intensification of tropical cyclones has been studied earlier with diagnostic models and with prognostic models that do not resolve convection. In this paper, a prognostic, axisymmetric model with explicit convection is used to study the effect of peripheral convection on tropical cyclone formation from a weak mesoscale vortex. Peripheral convection becomes stronger in the model if downdrafts extinguish deep convection in the core of the mesoscale vortex. The subsequent concentration of convection in the core of the vortex and the onset of rapid intensification of the vortex occur simultaneously. In model experiments, relative humidity in the midtroposphere reaches a value of 90% within 100 km from the center of the vortex before the onset of rapid intensification occurs.

Decreasing the sea surface fluxes of sensible and latent heat artificially in the outer region of the vortex decreases the amount of outer convection in the model. This results in an earlier onset of rapid intensification of the vortex into a tropical cyclone. By comparing model experiments with normal and artificially decreased sea surface fluxes in the outer region, the response to outer convection is shown to consist of an increase of tangential wind in the outer region, a decrease of tangential wind in most of the inner region in the boundary layer, and heating of the inner region. These changes are unfavorable for future inner convection. With weak inner convection, the important moistening of the inner region is retarded and the onset of rapid intensification is delayed. However, the inner convection's role in the moistening may be somewhat smaller than suggested by the model experiments if the mesoscale vortex is moistened while it forms. As the results suggest that the peripheral convection's detrimental effect for the intensification of the vortex is owing to its effect on the location of future convection, models that do not include convection as a process that responds to stability may severely underestimate the detrimental effects of peripheral convection.

The effect of the Coriolis parameter on the intensification depends on the strong downdrafts that severely weaken the inner convection. If the cooling by evaporation of precipitation is prevented in the model, inner convection remains strong and development of the mesoscale vortex into a hurricane occurs in less than 40 h for the value of the Coriolis parameter of both 10° and 30° latitude. When cooling owing to evaporation of precipitation is allowed and Coriolis parameter is that of 10° latitude, the small inertial stability in the outer region of the vortex results in little balanced response to the outer convection. The inner convection resumes relatively early and a tropical cyclone develops in 80 h from the start of the simulation. When the Coriolis parameter is that of 30° latitude, balanced response to the outer convection is stronger and the development of a tropical cyclone takes twice as long as at the latitude of 10°.

1. Introduction

Recent research has significantly improved understanding of those aspects of tropical cyclogenesis that depend on the interaction of mesoscale vortices (e.g., Wang and Holland 1995; Ritchie and Holland 1997; and Simpson et al. 1997) and axisymmetrization of convectively produced potential vorticity (PV) anomalies in the presence of a primary vortex (e.g., Montgomery and Enagonio 1998; and Möller and Montgomery 1999). In these studies convection has either not been accounted for directly or it is included with a conditional instability of the second kind (CISK)–type parameterization, in which convection does not depend on local instability but on relative vorticity. The direct effect of convective heating on the intensification of a vortex was studied by Shapiro and Willoughby (1982). They examined the direct response of hurricane-like vortices to sources of heat and momentum using Eliassen's (1951) diagnostic technique and showed that lower-tropospheric heat sources outside the radius of maximum wind can induce negative tendencies of tangential wind near the center. With sources at still larger radii, the negative tendencies of tangential wind extended even beyond the radius of maximum wind.

In a study of purely surface flux–driven polar lows, which bear close resemblance to tropical cyclones, Emanuel and Rotunno (1989) found that if an incipient polar low is too big, it will not intensify. They solved the Boussinesq form of the Sawyer–Eliassen equation

Corresponding author address: Marja Bister, Finnish Meteorological Institute, Meteorological Research, P.O. Box 503, FIN-00101 Helsinki, Finland.
E-mail: marja.bister@fmi.fi

in a vortex with constant vorticity to show that heating occurring outside some fraction of the deformation radius leads to a strong secondary circulation inside the radius of heating. This secondary circulation spins up a strong cyclone in the upper troposphere inside the radius of heating. The larger the radius of heating is, the more energy will be taken by the upper cyclone at the expense of the lower-level cyclone. They conclude that since the upper-level cyclone cannot feed back on the sea surface fluxes, the storm will not intensify.

Observations suggest that the radial location of convection is a rather good indicator of tropical cyclogenesis. Lunney (1988) studied differences between developing and nondeveloping tropical disturbances using data from U.S. Air Force northwestern Pacific aircraft reconnaissance flights. Defense Meteorological Satellite Program satellite data were used to determine any relationships between the amount and location of deep convection and low-level circulation centers that had been detected by the reconnaissance flights. The low-level circulation centers were rather small, about 50–100 km in radius. Convective elements were counted in each radial band for the developing and nondeveloping systems. Although the total amount of convection was larger within 4° of the center in nondeveloping cases, the ratio of convection within 2° of the center to that within 4° of the center was found to be 0.46 in developing cases and only 0.24 in nondeveloping cases.

Montgomery and Enagonio (1998) studied axisymmetrization of small-scale, convectively produced PV anomalies in the presence of a primary vortex. They showed that the asymmetrization occurs efficiently and leads to the spinup of the main vortex. However, when the axisymmetric convective forcing was made to occur too far from the radius of maximum wind, a slight spindown of the main vortex resulted.

Bister and Emanuel (1997, hereafter referred to as BE97) used the Rotunno–Emanuel model (described in section 2) to study development of a tropical cyclone from a cold-core mesoscale vortex that formed in the model owing to evaporation of stratiform precipitation. In simulations with increased intensity of stratiform precipitation or increased areal extent of the precipitation, convection developed in the outer regions of the evaporationally produced vortex as a result of increased wind and sea surface fluxes there. In one experiment, sea surface fluxes of latent and sensible heat were artificially prevented outside the radius of 340 km to decrease the amount of outer convection.[1] The resulting development was remarkably faster than in the case with sea surface fluxes allowed everywhere. However, the reason why outer convection was detrimental for the development was not studied.

Bister (1997) showed that the effect of the Coriolis parameter on the onset of rapid intensification of a mesoscale vortex depends on whether evaporation of rain is allowed to affect temperature. The maintenance and strength of peripheral convection in the model simulations depended on the existence of strong downdrafts in the inner region. It was suggested that peripheral convection can have a negative effect on the intensification via its effect on the location of future convection.

The goal of this work is to study the role of the peripheral convection in more detail. We assume that the mesoscale vortex has already formed and developed downward so that the vortex of the initial state has a warm core also in the lower troposphere. The organization of the paper is as follows. In section 2 the numerical model used in this study is described. In section 3, we discuss experiments to study the development of a tropical cyclone using different values of the Coriolis parameter with and without full effects of evaporation of precipitation. Particular attention is paid to the role of the outer convection in a higher-latitude case. In section 4, behavior with two different values of the Coriolis parameter is discussed in more detail. Section 5 contains discussion of the results and conclusions are given in section 6.

2. Numerical model

The model developed by Rotunno and Emanuel (1987, hereafter referred to as RE87) and modified by BE97 and Bister and Emanuel (1998) is used for the numerical experiments. The model is axisymmetric and nonhydrostatic, and resolves convection. The main modification made in BE97 was the inclusion of predictive equations for cloud water and rainwater mixing ratios using Kessler microphysics. Bister and Emanuel (1998) added dissipational heating to the model. Dissipational heating was found to increase the maximum wind of the mature system by about 20%. The maximum dissipational heating in the boundary layer in a mature hurricane in the current simulations exceeds 100 K day^{-1}.

As discussed in RE87, simulating the radiative convective equilibrium with a two-dimensional model may lead to artificial development because turbulence is restricted to occur in two dimensions. Therefore, we do not include any mean wind and we simulate radiation with Newtonian cooling to minimize the amount of turbulence. The maximum magnitude of cooling, or warming in case of a cold anomaly, is set of 2 K day^{-1}. The initial sounding is also the same as that in RE87 and is nearly neutral to model's convection.

In each of the experiments, the model is initialized with a warm-core vortex with a maximum wind speed of 8 m s^{-1} at the radius of 94 km. The initial tangential

[1] By peripheral and outer convection we mean convection occurring well outside the radius of maximum wind of the vortex. Note also that the strong convection occurring far from the radius of the maximum wind in the model of BE97 was at least partly an artifact of not simulating the radiative convective equilibrium.

wind vanishes at the radius of 416 km. The structure of the initial vortex is that given in RE87 with one modification. Since the radial variation of the initial tangential wind speed depends on the Coriolis parameter and we are interested in the effect of varying the Coriolis parameter, we decided to use a common value of 5×10^{-5} s^{-1} in the vortex specification in all of the experiments. Two simulations were conducted with the value of the Coriolis parameter of 7.5×10^{-5} s^{-1} elsewhere than in the vortex specification. In the vortex specification either 7.5×10^{-5} s^{-1} or 5.0×10^{-5} s^{-1} was used. The results were similar, suggesting that the modification in the specification of the vortex did not affect the results.

Since we use a rather weak initial vortex, convective downdrafts prevent convection from resuming in the core of the vortex for a longer period than they presumably would with a stronger initial vortex. As a result, the strongest convection can often be found quite far from the center. Thermodynamic changes associated with this convection occurred too close to the original location of the outer boundary which was 1500 km from the center. When the outer boundary was moved to 4500 km from the center, the disturbance developed somewhat faster. Moving the outer boundary still further did not affect the results. Hence, the outer boundary was set to 4500 km. The upper boundary is at the height of 30 km. Horizontal grid spacing of 7.5 km and vertical grid spacing of 1.25 km are used.

At some time instances the strongest vertical velocity occurs in the center very close to the base of the model's sponge layer, which is at the height of 24.375 km, and does not reflect deep convection directly below. This feature raised concern that the upper boundary condition might affect the simulation. However, when small modifications that should be of small meteorological influence were made to the model, the upper vertical velocities varied greatly and still the results were similar to the control simulation's results. Hence, these vertical velocities, whether associated with the upper boundary condition or not, did not seem to affect the simulations.

3. Dependence of the intensification on the peripheral convection

The four basic experiments start with the same initial condition described in section 2. In simulation TR (Tropics) the Coriolis parameter is 2.5×10^{-5} s^{-1}, corresponding to the latitude of 10°. In simulation ST (subtropics) the Coriolis parameter is 7.5×10^{-5} s^{-1}, corresponding to the latitude of 30°. Experiments TRNE and STNE are similar to TR and ST, respectively, but the cooling associated with evaporation of precipitation is set to zero. Evaporation is still allowed to turn rain into water vapor.

The maximum tangential wind speed in the four experiments is shown in Fig. 1. In experiment TR, the weak vortex intensifies into a hurricane in 80 h. The intensification takes twice as long in experiment ST. However, if evaporation of precipitation is not allowed to affect temperature, the weak vortex intensifies into a hurricane in less than 40 h at both latitudes. Hence, the value of the Coriolis parameter affects the intensification significantly only if evaporation of precipitation is allowed to affect temperature. The fifth contour in Fig. 1, labeled with ''20deg,'' is for the experiment in which the Coriolis parameter is 5×10^{-5} s^{-1}, which is the mean of the values in experiments ST and TR. The onset of rapid intensification in this experiment occurs at a time that is the mean of the corresponding times in experiments ST and TR. In the following, we will study experiments ST, TR, STNE, and TRNE more closely.

Evaporation of precipitation causes downdrafts that have a strong influence on the location of further convection. In experiment ST, for example, convection starts about 20 h after the beginning of the experiment (hereafter, times are always given from the start of the experiment) and during 20–24 h there is convection from the radius of 50 to 70 km (not shown). After 4 h, equivalent potential temperature in the boundary layer, $\Theta_{e,bl}$, has dropped by 9 K in this region and convection has spread inward and outward from the same region. During the next 4 h (28–32 h), $\Theta_{e,bl}$ has a negative anomaly compared to its initial value between the radii of 30 and 140 km, excluding the ring between 100 and 110 km. At this time, convection occurs within the radius of 25 km and from the radius of 120 to 180 km. During the next 12 h (32–44 h) convection is much stronger outside the radius of 180 km than within. Toward the end of this period, $\Theta_{e,bl}$ has been replenished inside the radius of 160 km and during the next 4 h convection strengthens within the inner 100 km. Later in this section, we will study the budget for $\Theta_{e,bl}$, which confirms that before the rapid intensification, downdrafts have a strong effect on $\Theta_{e,bl}$.

The relative strength of convection at different radii is shown in Figs. 2 and 3.[2] Figure 2 shows the location of the strongest instantaneous vertical velocity below the height of 16.875 km as a function of time in the four experiments. In experiments STNE and TRNE, the strongest convection occurs mostly within the inner 50 km until the storm has reached a mature state. In contrast, in experiments TR and ST the strongest convection occurs quite often far from the initial radius of maximum wind after 30 h. In experiment TR, the outer convection stops dominating the inner convection in strength by 70 h, at which time rapid intensification of the vortex starts (Fig. 1). In experiment ST, the strongest convection

[2] Note that in Figs. 3 and 6 area averaging is used even though averages over area are more affected by the inexact definition of the radius dividing the integration domain into inner and outer regions. However, averages over radius were mostly qualitatively similar to the averages over area (not shown).

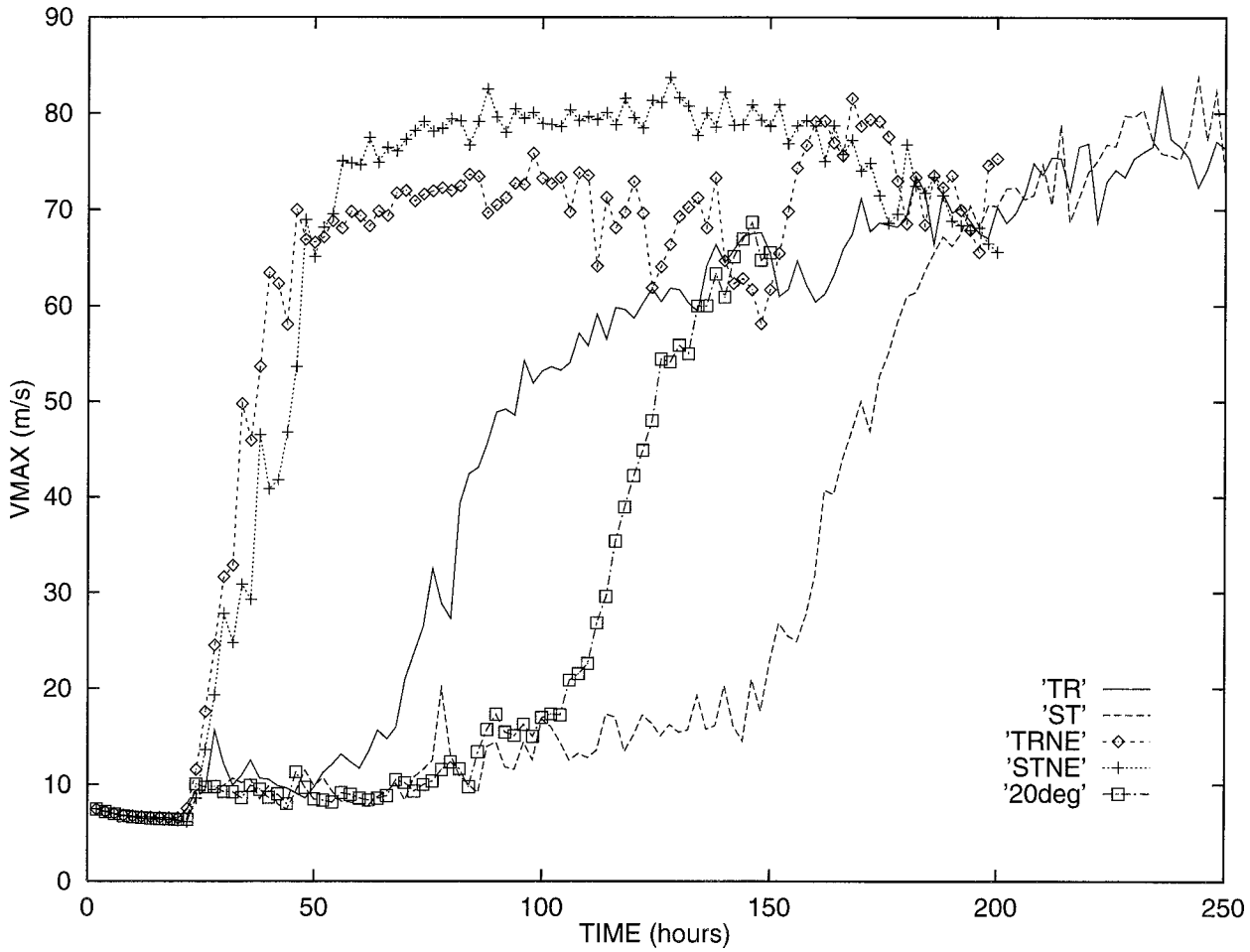

FIG. 1. Maximum tangential velocity as a function of time in experiments TR, ST, TRNE, STNE, and 20°.

stops occurring hundreds of kilometers from the center and can be found at or within the inner 100 km when rapid intensification starts at around 150 h.

In Fig. 3, the average mixing ratio of rainwater within the radius of 100 km and from the radius of 100 to 300 km is shown for experiments ST and TR. Note that the values for the latter region have been multiplied by 10. Note also that the area of the latter region is about eight times as big as the area of the former region. In experiment ST, the outer convection weakens significantly when the inner convection experiences rapid strengthening, which occurs simultaneously with the rapid intensification of the vortex from 150 to 200 h. In experiment TR, the behavior of outer convection is more variable in time than in experiment ST. Still, there is little outer convection during the rapid strengthening of inner convection also in experiment TR, except around 100 h.

It is interesting that the onset of rapid intensification of the vortex and the concentration of convection in the inner region occur almost simultaneously in both TR and ST, which is shown by comparison of Figs. 1 and 3. Although the maximum tangential wind speed increases slightly in experiment ST even before the concentration of convection occurs at around 150 h, rapid intensification in both experiments ST and TR only occurs when the inner convection dominates the outer convection whether in terms of maximum vertical velocity or area-averaged rain mixing ratio (Figs. 1–3). Montgomery and Enagonio (1998) have also shown that the location of a convectively produced potential vorticity anomaly greatly affects the spinup rate of a weak vortex, with the anomaly occurring closer to the center causing greater spinup than the anomaly occurring farther from the center outside the radius of maximum wind.

What is the trigger for the concentration of convection in the inner region that starts around 70 and 150 h in experiments TR and ST, respectively? Initially, downdrafts associated with convection bring low-Θ_e air into the boundary layer preventing convection in the same location until replenishment of $\Theta_{e,bl}$ has occurred, as discussed above. Moistening of the inner region might reduce evaporation of precipitation leading to weaker downdrafts there. Thus convection might be maintained in the inner region and intensification of the vortex into hurricane strength could be possible.

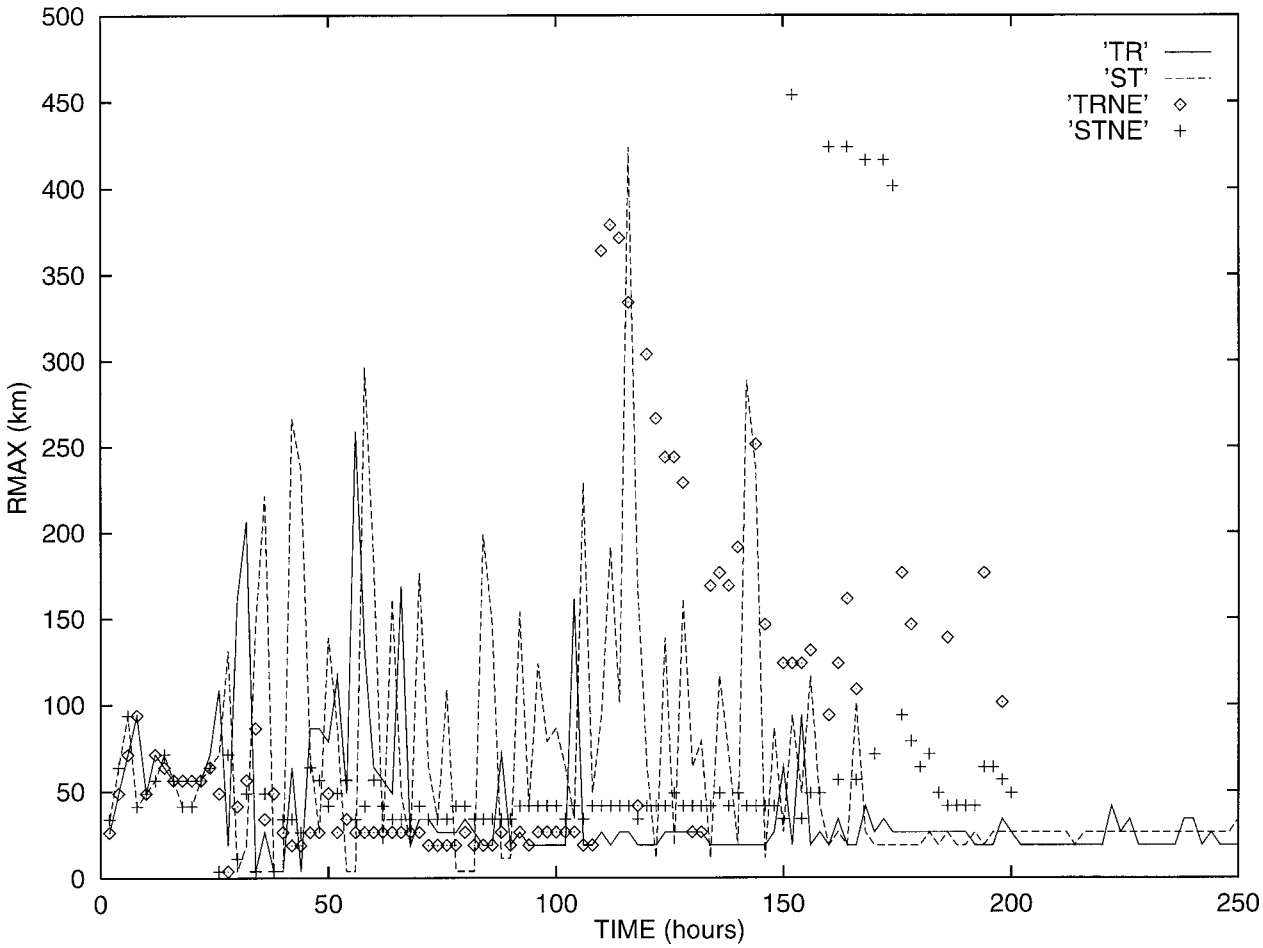

FIG. 2. Radius of the maximum vertical velocity as a function of time in experiments TR, ST, TRNE, and STNE. Between 140 and 200 h, the strongest convection in experiment TRNE occurs often in the radial band from 700 to 1300 km, which is outside the domain plotted.

Figure 4 shows the relative humidity averaged from the center to the radius of 100 km, and from the height of 0.625 to 5.625 km. In experiments TR and 20deg, the rapid concentration of convection and the rapid intensification of the vortex (Fig. 1) begin when the averaged relative humidity reaches a value of 90%. This occurs after 65 h in experiment TR and after 100 h in experiment 20deg. In experiment ST, relative humidity hovers at a value slightly less than 90% for about 40 h before the rapid intensification starts. Figure 4 suggests that the inner region must be very humid before the rapid intensification can start. The moistening is due to convection, which always exists somewhere within the inner 100 km after the first 20 h (Fig. 3). Ekman pumping also contributes to the moistening.

Using a simple axisymmetric model, Emanuel (1989) found that the time of onset of intensification of a warm-core vortex depends strongly on the midtropospheric humidity. Simulations with a modified version of the same model (Emanuel 1995) suggested that the near saturation of a mesoscale column of the troposphere at the cyclone core is a necessary condition for intensification. The rapid strengthening following the moistening of the midtroposphere was explained by Emanuel: ''Only when the troposphere is nearly saturated are the downdrafts that normally accompany deep convection suppressed; this allows surface fluxes to actually increase the entropy of the subcloud layer and, along with it, the temperature of the troposphere.'' Observational support for the importance of the moistening was obtained from Tropical Experiment in Mexico (BE97). Observations showed a cold-core vortex with a small positive temperature anomaly in its center. The averaged relative humidity in the region of the vortex reached a value of 85% at the altitude of 3 km. After about a day the system reached hurricane strength.

We conducted two experiments to study the effect of varying the initial humidity in the region of the mesoscale vortex. The same value of Coriolis parameter was used as in experiment ST. In one experiment, relative humidity was set equal to 90% and in the other 20% within the inner 100 km from the height of 1.875 to 6.875 km. In changing the relative humidity, temperature was adjusted so as to conserve the virtual tem-

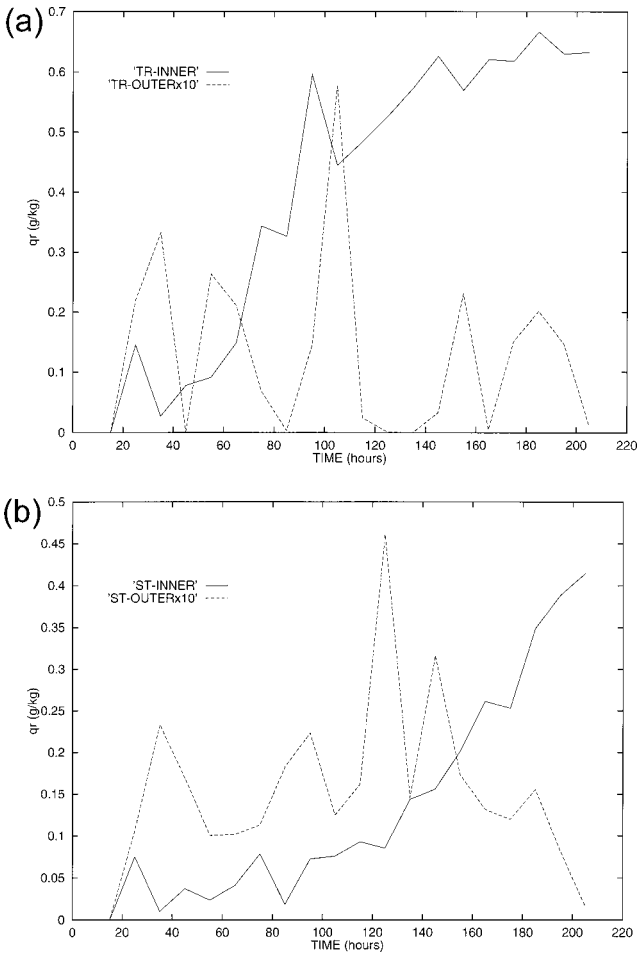

FIG. 3. Area-averaged mixing ratio of rainwater (g kg^{-1}) within the radius of 100 km and from the radius of 100 to 300 km in experiments (a) TR and (b) ST. The values are 10-h averages and have been calculated for a layer from the height of 0.6 to 5.6 km. The values from the radius of 100 to 300 km have been multiplied by 10.

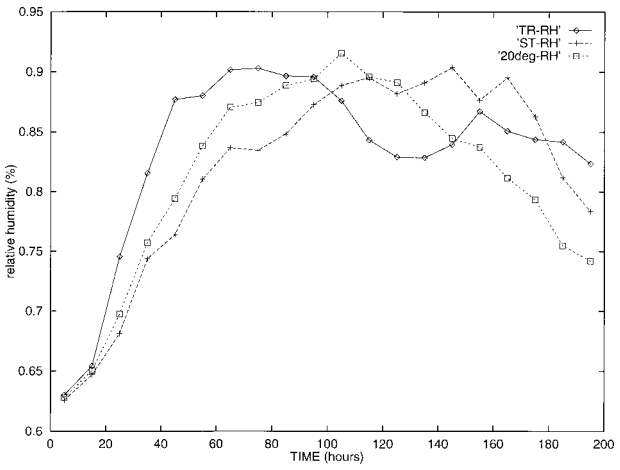

FIG. 4. Relative humidity within the inner 100 km in experiments TR, ST, and 20°. Averages are taken over radius.

perature. The behavior of the maximum tangential velocity in the two experiments is shown in Fig. 5. The vortex with relative humidity of 20% fails to intensify into a hurricane within the first 300 h. The vortex with relative humidity of 90% intensifies even more rapidly than the vortex in experiment TR (Fig. 1). In the experiment with 90% relative humidity, the rain mixing ratio is more than twice that in experiment ST within the inner 100 km until the rapid intensification begins in the former (not shown). Until about 30–40 h, there is as much outer convection in these two experiments. Later, there is a decreasing trend in the amount of outer convection in the experiment with 90% relative humidity, whereas in experiment ST there is an increasing trend until 120 h. In both experiments, the short-term variations in the strength of outer convection are very large.

In the rest of this section, we will study the model experiments ST, TR, STNE, and TRNE more closely to understand how the outer convection is able to remain strong in the simulations and, more importantly, what its role is in the intensification of the weak mesoscale warm-core vortex into a hurricane. In experiment TRNE, there is very little outer convection until the system has reached a mature state (Fig. 6). In experiment STNE, outer convection exists at around the radii of 120 and 150 km around 35 h (not shown). Ten hours later, outer convection weakens while the inner convection intensifies rapidly (Fig. 6). The strong inner convection that is little affected by downdrafts seems to prevent sustained outer convection in these experiments while the intensification of the vortex occurs. This could be due to radial advection of low-Θ_e air that balances the sea surface fluxes of heat thereby preventing the local increase of Θ_e to values that could sustain convection. The rather strong inward velocity associated with the circulation that distributes the heating (Breth-

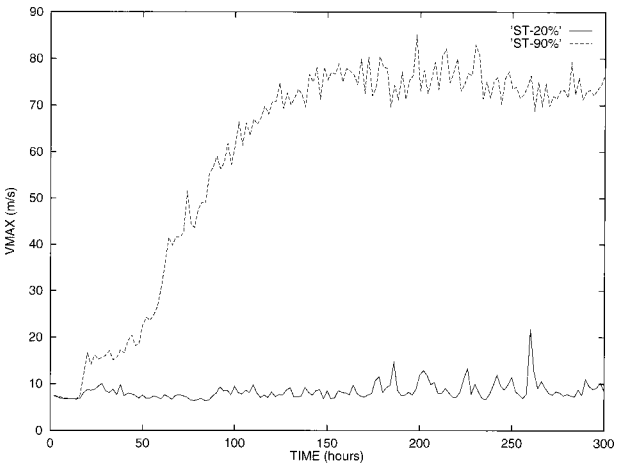

FIG. 5. Maximum tangential velocity in experiments similar to ST but with initial humidity set to 20% and 90% within the inner 100 km and from the height of 1.9 to 6.9 km.

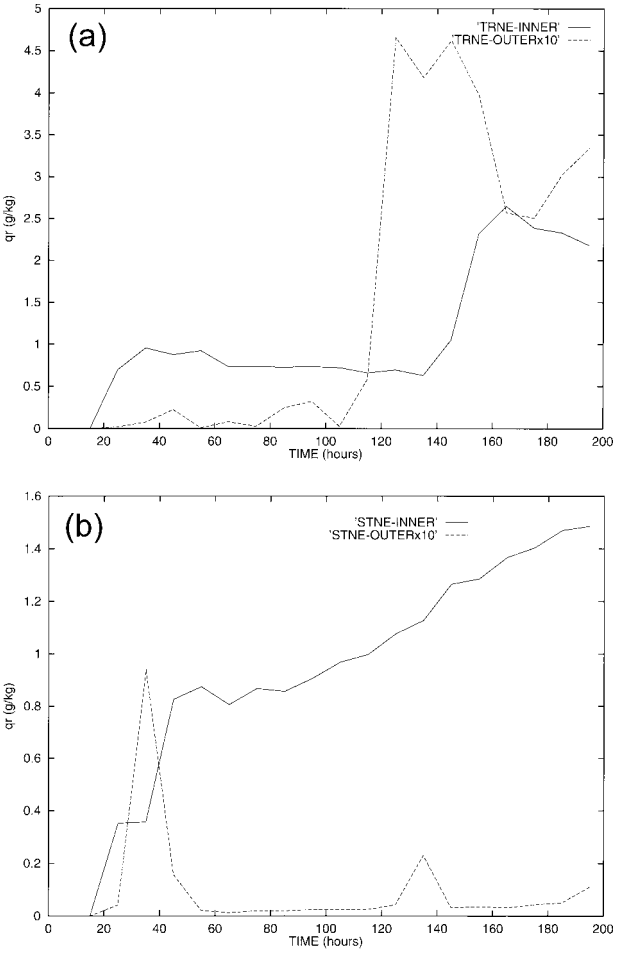

FIG. 6. Same as Fig. 3 but for experiments (a) TRNE and (b) STNE.

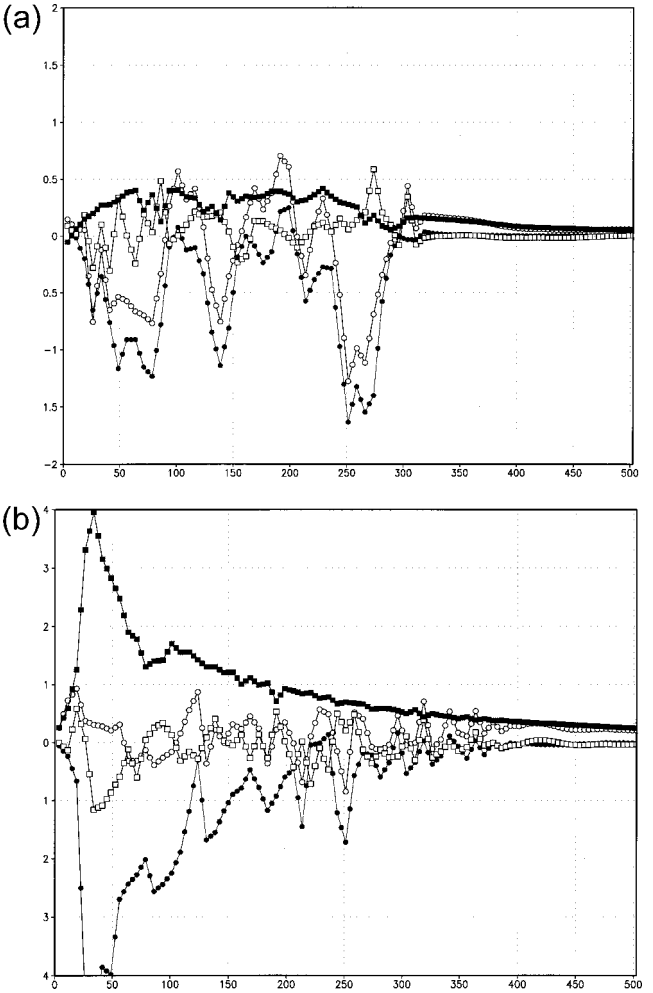

FIG. 7. The Θ_e budget in the boundary layer for experiment (a) ST and (b) STNE; tendency (open circle), horizontal advection (filled circle), vertical advection (open square), vertical diffusion (filled square). The *x* axis shows the radius (km) and the *y* axis shows the heating rate (°C h^{-1}).

erton and Smolarkiewicz 1989) occurring in the inner core could be expected to stop gradually if the inner convection stopped. Already between 30 and 40 h the radial inward velocity of 4 m s^{-1} extends to the radius of 240 km in the boundary layer in experiment STNE. In contrast to experiments STNE and TRNE, experiment ST shows that between 18 and 28 h the boundary layer Θ_e has decreased by almost 10 K between the radii of 45 and 90 km. When the inner convection dies due to the adverse effects of the downdrafts, outer convection intensifies.

To study this effect, we calculate the $\Theta_{e,bl}$ budget for experiments ST and STNE between 40 and 50 h. This is done similarly as in RE [see their Eqs. (38)–(42)]. Figure 7 shows the three leading terms of the budget: horizontal advection, vertical turbulent diffusion, and vertical advection as well as the local tendency of $\Theta_{e,bl}$. The remaining terms, horizontal turbulent diffusion and radiation, are typically much smaller than the other three terms. In experiment ST, horizontal advection is mostly negative. It is often the largest term and dominates the tendency. In STNE, horizontal advection and vertical turbulent diffusion, which includes the sea surface transfer of Θ_e, are the largest terms. However, horizontal advection has a contribution from the spreading of cold and dry downdrafts in the boundary layer. To quantify the contribution from the mean circulation, we calculate

$$\overline{u}\frac{\partial}{\partial r}\overline{\Theta}_e,$$

where the overbar denotes average over 10 h, from 40 to 50 h. In the region from the radius of 120 to 300 km,[3] the mean circulation accounts for 60% of the horizontal advection in experiment STNE but only 20% in experiment ST. This supports the view that in the presence of strong sustained inner convection, as in exper-

[3] The averaging region was chosen so as to exclude the ring from 100 to 120 km, since some convection still occurred in this ring in experiment STNE between 40 and 50 h.

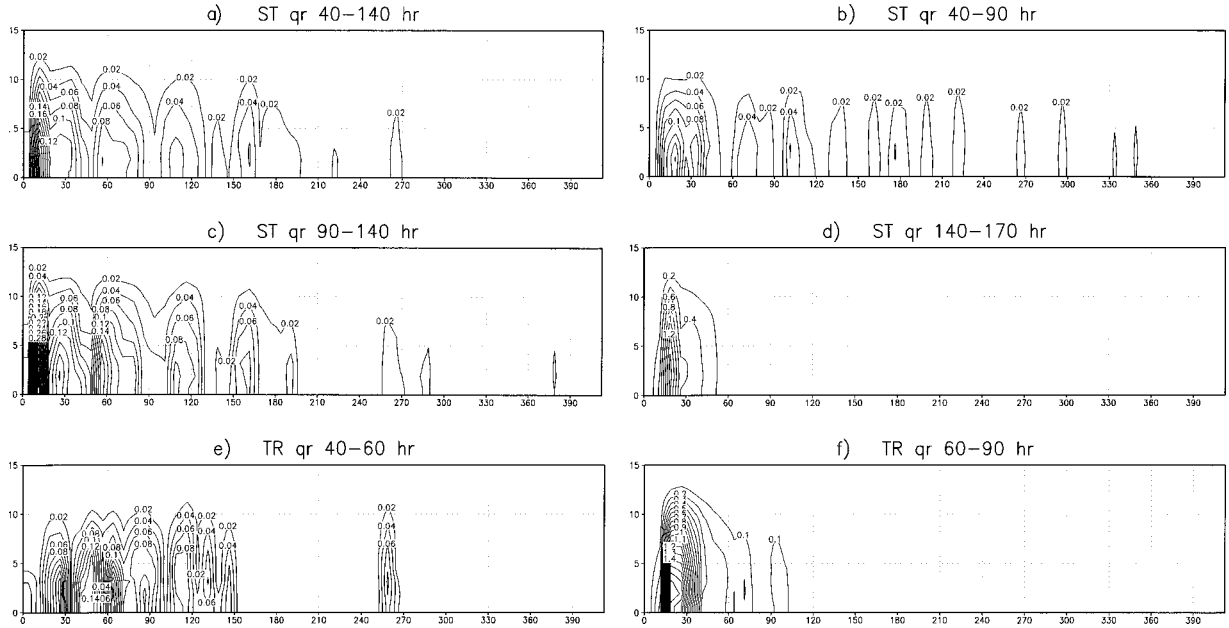

FIG. 8. Mixing ratio of rainwater (g kg^{-1}) as a function of radius and height (km) averaged between times shown: (a)–(d) experiment ST; (e) and (f) experiment TR.

iment STNE, the associated mean radial circulation has a large, negative effect on the $\Theta_{e,bl}$ budget. In experiment ST, the horizontal advection is typically negative and it takes negative maxima at around 140 and 250 km. The negative maxima are likely owing to spreading convective downdrafts there, which is supported by the location of convection at this time (not shown).

The relative strength of the outer convection as compared to the inner convection can be seen in Fig. 8. The convective development in experiment ST can be divided into three periods, of which the first two occur before the rapid intensification starts at around 140 h (Fig. 8a). During the first period, outer convection occurs in a large range of radii (Fig. 8b). During the second (Fig. 8c), outer convection mostly occurs within the inner 200 km. During the third period, when the rapid intensification occurs, the inner convection clearly predominates (Fig. 8d). The average of the first and the second periods is shown in Fig. 8a. The averaging makes the outer convection look rather weak compared to convection within the inner 20 km. In the outer region, the location of convection varies greatly in time, resulting in a rather smooth field of averaged rain mixing ratio. The averaged rain mixing ratio is largest within the inner 20 km because convection can be found more often in this place than in any other place. However, the mean rain mixing ratio in the outer region (Fig. 8a), although being smaller, occurs over a very large area, making it important in an integrated sense. In experiment TR, convection occurs between 20 and 150 km and close to 260 km in radius before rapid intensification takes place (Fig. 8e). During the time of rapid intensification, between 60 and 90 h, convection is concentrated to the band from 15 to 40 km in radius (Fig. 8f).

In simulations of BE97, discussed in section 1, peripheral convection was detrimental for the development of a cold-core vortex into a hurricane. This combined with the prominence of the peripheral convection in experiment ST suggests that outer convection may prevent the rapid intensification of a weak mesoscale vortex from occurring as early as it would in the absence of outer convection. A possible mechanism, suggested by Bister (1997), is that the outer convection increases locally the tangential wind speed due to conservation of angular momentum necessitating an adjustment inside the radius where tangential wind increases. First, if the inner wind does not change, the wind increase in the outer region must lead to an increase in the inner temperature, which can be seen by integrating the gradient wind law over radius and using the hydrostatic law. Second, if the inner temperature does not change, the wind increase in the outer region must be associated with a decrease of the pressure gradient between the outer region and the inner core, leading to a decrease in the low-level tangential wind speed and surface heat fluxes there. The local tangential wind increase associated with the outer convection is expected to lead to a balanced response that consists of a secondary circulation anomaly with subsidence in the inner core and outward motion in the lower troposphere. These changes lead to warming and decrease of the lower-tropospheric wind in the inner core. Both factors suppress development of convection in the inner core, thereby slowing

down the moistening of the inner core and the development of the vortex into a hurricane.[4]

To study the role of the outer convection, a simulation should be made in which the outer convection is prevented from occurring. A few experiments were made in which the diabatic heating owing to convection was set to zero outside a fixed radius. However, this lead to an unrealistic situation with very strong and persistent convection just inside the critical radius. Since the inflowing air could not convect at all in the absence of latent heating, convective available potential energy (CAPE) accumulated and resulted in strong convection just inside the critical radius.

A more sensible way to mitigate the outer convection is to decrease or to prevent sea surface fluxes of latent and sensible heat in the outer region. The drawback of this approach is that the inner convection may also be affected due to decreased Θ_e of the inflowing air. Keeping this dual role of the artificial decrease of the sea surface fluxes in mind, we conducted an experiment, STSSF, which is similar to experiment ST but the sea surface fluxes were set to zero outside the radius of 184 km. This prevents strong outer convection from occurring outside the radius of 150 km as shown in Fig. 9b. This can also be seen from plots of time-averaged vertical velocities (not shown). Indeed, the system intensifies 14 h earlier than when the sea surface fluxes of heat are allowed at all radii (Fig. 9a). Although this time difference is not very large, it is remarkable that the system with smaller sea surface fluxes in the outer region intensifies more rapidly than the system with larger sea surface fluxes showing that the location of convection can be more important than the overall amount of convection. The result of more rapid intensification in the presence of decreased sea surface fluxes is remarkable considering the general dominant role of the sea surface fluxes in hurricane intensification and maintenance (Ooyama 1969; Emanuel 1986; and RE87).

The mature hurricane in STSSF is weaker than in ST (Fig. 9a). This is probably due to a negative effect that decreasing sea surface fluxes has on the inner convection. Figure 10 shows the difference of relative humidity in experiments STSSF and ST just before, during, and after the rapid intensification in STSSF. The outer domain is remarkably drier in STSSF in the boundary layer and especially in the midtroposphere. The small relative humidity in the midtroposphere is probably mostly due to the lack of outer convection. The small relative humidities in STSSF extend to the core of the vortex during the rapid intensification and probably cause the leveling off of the maximum tangential wind after 150 h in that experiment (Fig. 9a). It can be speculated that, in reality, convection and stratiform precipitation in and close to the region where the mesoscale vortex will form would moisten the midtroposphere so that the role of outer convection in the moistening of the midtroposphere would be less significant *after* the mesoscale vortex has formed.

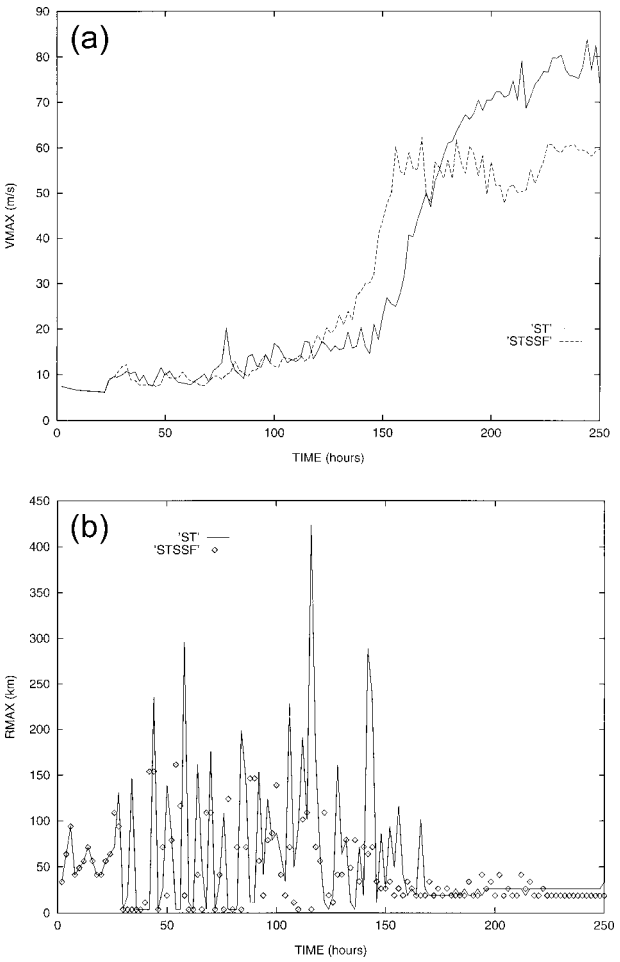

FIG. 9. (a) Maximum tangential velocity and (b) radius of the maximum vertical velocity as a function of time in experiments ST and STSSF.

It is instructive to look at the differences of the developing vortex in experiments ST and STSSF. Figure 11 shows slightly smoothed and time-averaged differences of tangential wind, mixing ratio of rain, saturation Θ_e, and pressure before the rapid intensification begins in experiment STSSF. Except within the innermost 45 km, the tangential wind in the boundary layer is smaller within and larger outside the radius of 190 km in ST than in STSSF. The mixing ratio of rain in experiment ST is larger outside the radius of 150 km and smaller in most regions within this radius (except in most of the inner 40 km) than in experiment STSSF. Also, ST

[4] Note that the aforementioned hypothesis bears close resemblance to both the original hypothesis of Project Stormfury, namely, that heating in the outer region would decrease the pressure gradient inside the region of heating; and to the revised hypothesis of Sundqvist (1970) and Rosenthal (1971), that when the radius of maximum heating is larger than the radius of maximum wind, the maximum wind speed decreases through conservation of angular momentum. However, the Stormfury hypotheses did not consider the effects of heating on the location of future convection.

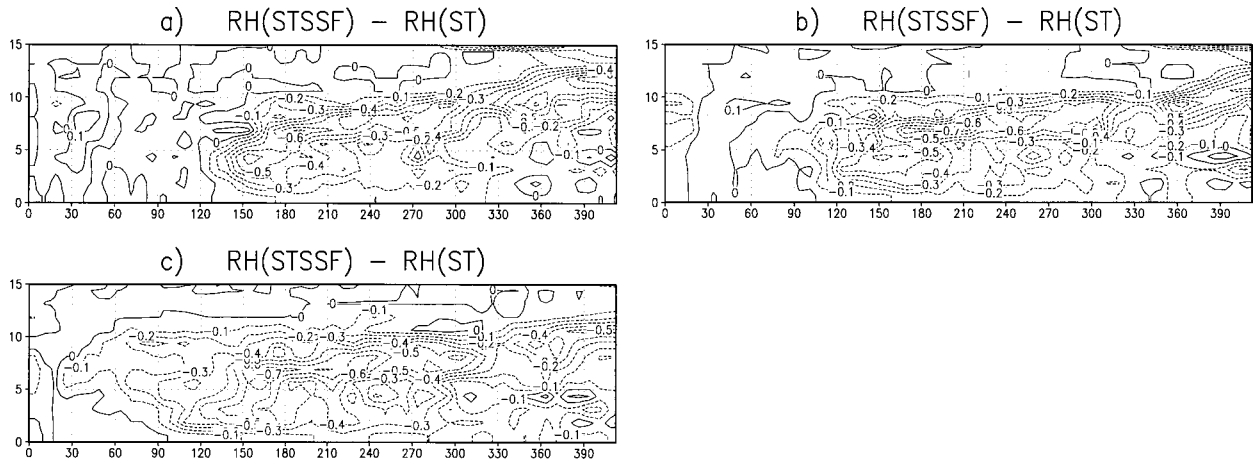

FIG. 10. Difference of relative humidity (%) in experiments STSSF and ST as a function of radius and height (km) averaged between (a) 110 and 130 h, (b) 130 and 150 h, and (c) 150 and 170 h.

is warmer than STSSF in almost the whole inner 150 km and the surface pressure is smaller in ST than in STSSF. Even though saturation Θ_e, which is a temperature variable, is larger and surface pressure is smaller in ST than in STSSF, the onset of intensification occurs later in ST than in STSSF.

Except for the inner 40 km or so, where the tangential velocity and the mixing ratio of rain are larger in experiment ST than in experiment STSSF, the differences between experiments ST and STSSF support our hypothesis concerning how outer convection delays the onset of rapid intensification. Namely, the larger amount of outer convection in experiment ST leads to a stronger tangential wind in the outer region and a weaker tangential wind in the inner region, and a warmer inner region. These changes weaken the inner convection and thereby slow down the moistening of the inner region and the intensification of the vortex.

4. Effect of Coriolis parameter on peripheral convection and intensification

Figure 1 suggests that the Coriolis parameter has a minimal effect on the intensification when evaporation of precipitation is not allowed to affect the temperature. In the presence of very weak downdrafts, the strongest convection occurs in the inner core until the vortex has intensified into a mature state hurricane (Fig. 2). Intuitively, the reason why the value of the Coriolis parameter does not affect these simulations is that when convection stays inside the radius of maximum wind, inertial stability (e.g., Schubert and Hack 1982) is dominated by the relative vorticity. However, when the outer convection develops in experiments ST and TR, the response depends on the Coriolis parameter, since outside the radius of maximum wind the Coriolis parameter's contribution to inertial stability is significant. The

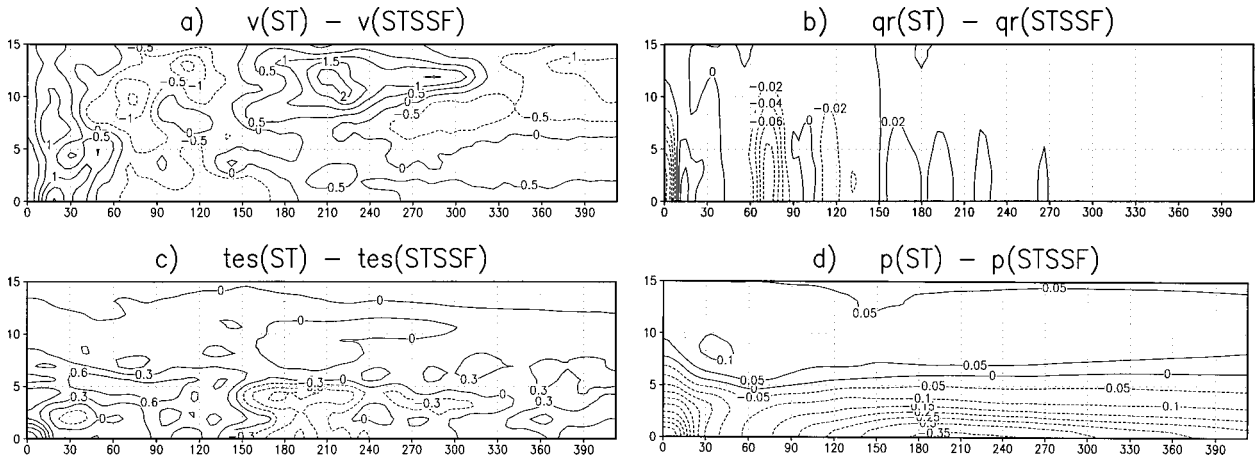

FIG. 11. Difference of (a) tangential wind speed (m s^{-1}), (b) mixing ratio of rainwater (g kg^{-1}), (c) saturation Θ_e (K), and (d) pressure (hPa) as a function of radius and height (km) in experiments ST and STSSF averaged between 30 and 120 h. Slight smoothing has been applied.

TABLE 1. Rossby radius of deformation for initial state of experiments ST and TR at different radii.

Expt	r = 70 km	r = 200 km	r = 300 km
TR (10°)	156	600	1590
ST (30°)	123	288	394

relative difference (difference of the two values divided by the mean of the two values) of initial inertial stability between experiments ST and TR is 46% at the radius of 70 km, 124% at the radius of 200 km, and 176% at the radius of 300 km. The corresponding Rossby radii of deformation, defined as the gravity wave speed divided by the square root of the inertial stability, are given in Table 1. A value of 30 m s^{-1} is used for the gravity wave speed. Note that the Rossby radii for experiment ST and TR are rather similar at the radius of 70 km but very different at the radii of 200 and 300 km. The Rossby radius of deformation gives a length scale over which gravity waves are damped. Thus convective heating is deposited within a horizontal dimension of the order of Rossby radius (see Emanuel 1994, 332–334; and Bretherton and Smolarkiewicz 1989).

The different structure of the vortices in experiments ST and TR before the rapid intensification starts in experiment TR is shown in Fig. 12. As the sizes of the vortices are similar (not shown), the differences are not related to size differences. Except in a small region within about 25 km from the center, the boundary layer tangential wind is smaller in experiment ST than in experiment TR within the radius of 105 km. The opposite is true outside the radius of 105 km. Still, saturation Θ_e is larger in ST implying that the boundary layer Θ_e must be larger in ST for convection to occur. Note that in the beginning of the simulation, the maximum difference in the saturation Θ_e between these two experiments is only 0.35 K (not shown). Hence, the difference in Fig. 12c does not just reflect the initial difference. Since the average maximum tangential wind between 40 and 60 h is slightly larger in experiment TR than in experiment ST (Fig. 1), the increase of the saturation Θ_e difference between experiments ST and TR in time is probably due to a different radial structure of the wind field in the two experiments. The largest saturation Θ_e difference between the two experiments can be found inside the radius of 120 km. The weaker wind speed in experiment ST than in experiment TR between the radius of 25 and 105 km implies smaller sea surface fluxes of heat there in experiment ST. Smaller sea surface fluxes of heat combined with larger saturation Θ_e within the inner region in experiment ST implies that convection is more unlikely to occur in that region in experiment ST than in experiment TR. In fact, the mixing ratio of rain shows that there has been less convection inside 120 km in ST than in TR except in one small region. Note, however, that the stronger inner convection in experiment TR than in experiment ST may also be augmented by differences in Ekman pumping. Ekman pumping is larger for smaller values of the Coriolis parameter. The associated larger moistening decreases the strength of the downdrafts within the inner core and favors the occurrence of the inner convection in experiment TR as compared to experiment ST.

In addition to the different effect of the outer convection in ST and TR owing to different inertial stability in the outer region, the *amount* of outer convection is significantly different in experiments ST and TR after the onset of rapid intensification in experiment TR. The averaged rain mixing ratio in a ring from 100 to 300 km from the center and between the altitudes of 0.6 and 5.6 km is on the mean almost twice as large in experiment ST as in experiment TR from 60 to 150 h. This may be due to two factors. First, the balanced response to the outer convection in ST increases tangential wind speed in the outer region locally and thereby also increases sea surface fluxes there, leading to more outer convection.

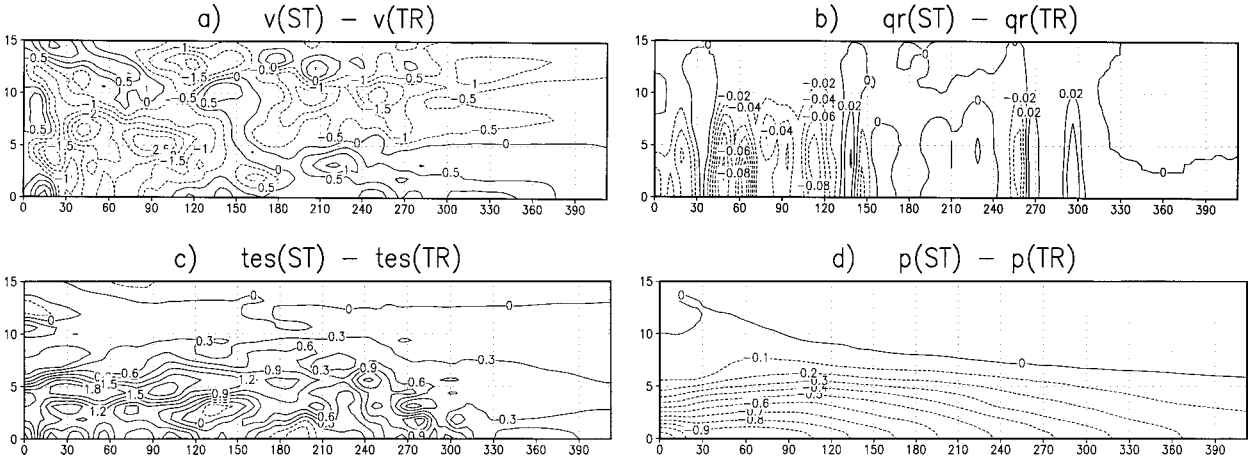

FIG. 12. Difference of (a) tangential wind speed (m s^{-1}), (b) mixing ratio of rainwater (g kg^{-1}), (c) saturation Θ_e (K), and (d) pressure (hPa) as a function of radius and height (km) in experiments ST and TR averaged between 40 and 60 h. Slight smoothing has been applied.

Second, the fact that there is no sustained inner convection in experiment ST may make it easier for the outer convection to occur, as discussed in section 3.

The mature state hurricanes in experiments ST and TR are rather similar (not shown). However, the hurricane in ST has over 10% larger maximum anomalies of pressure and temperature. In the boundary layer, the tangential wind speed in most of the region within the inner 400 km is somewhat larger (1–2 m s^{-1}) in experiment ST than in experiment TR. The largest differences in the tangential wind speed can be found in the outflow layer, where the wind is more anticyclonic in experiment ST. The secondary circulation is weaker in ST than in TR by about 20%–30%.

5. Discussion

In the numerical model, development of a weak warm-core mesoscale vortex into a hurricane takes twice as long with the value of the Coriolis parameter of 7.5 $\times$ 10^{-5} (30°) as with the value of 2.5 $\times$ 10^{-5} (10°). Both Khain (1984) and DeMaria and Pickle (1988) have shown with a numerical model that the development into a hurricane is slower for a higher value of the Coriolis parameter within certain bounds. The former attributed the slower intensification to the warmer temperature anomaly associated with a fixed vortex at higher latitude. The latter explained that the inflow extends closer to the center of a low-latitude vortex and therefore the intensification occurs sooner. We have shown that if evaporation of precipitation is not allowed to affect the temperature, development of a mesoscale vortex into a hurricane in the axisymmetric numerical model occurs as rapidly for both values of the Coriolis parameter. In the absence of evaporation's effect on temperature, strongest convection can be found at around the radius of maximum wind, and significant outer convection develops only when the vortices have developed into a mature hurricane. This result is qualitatively consistent with the results of Shapiro and Willoughby's (1982) diagnostic study. They showed that with the imposed heat source at the eyewall, changing the inertial stability in the outer region resulted in virtually no change.

As discussed in section 1, Emanuel and Rotunno (1989) found that heating occurring outside some fraction of the deformation radius in a polar low leads to a secondary circulation that spins up a strong cyclone in the upper troposphere inside the radius of maximum heating. It is interesting that the difference of tangential velocity in experiments ST and TR (Fig. 12) shows that just inside the radius where the boundary layer tangential wind is larger in ST than in TR in the region of the peripheral convection, tangential velocity in the upper troposphere is larger in experiment ST than in experiment TR. However, the magnitude of the difference is larger in the boundary layer than in the upper troposphere suggesting, that the spinup of the upper cyclone is not the reason why the intensification of storm is slower in experiment ST than in experiment TR.

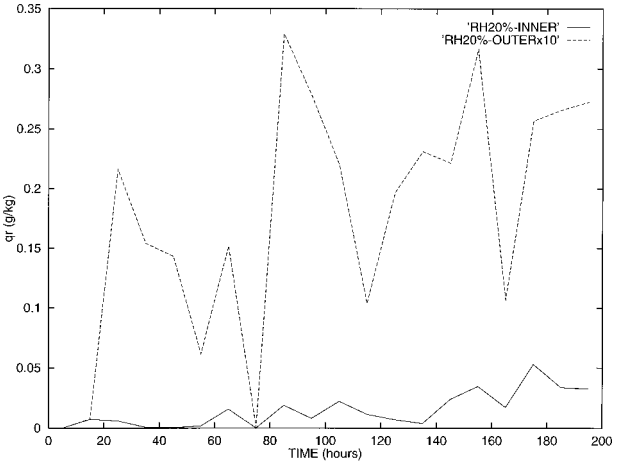

FIG. 13. Same as Fig. 3b but for experiment with initial relative humidity of 20% within the inner region. See text for details of this experiment.

Increasing the inertial stability by increasing the value of the Coriolis parameter delays the intensification of a weak mesoscale vortex in the model. Could the presence of a large-scale vortex have a similar effect? A sufficiently large vortex could add an almost constant value of vorticity in the whole region of the mesoscale vortex. However, increasing planetary vorticity decreases Ekman pumping, whereas increasing relative vorticity increases it. This affects the moistening of the inner region of the vortex. Also, the wind associated with the relative vorticity could have effects on the magnitude and radial location of convection via increased sea surface fluxes. Yet, another difference is that a large-scale vortex may be associated with an anomaly in the midtropospheric moisture. On the other hand, as shown by McBride and Zehr (1981), the moisture of the midtroposphere does not correlate with cyclogenesis and an explanation for this surprising observation has been suggested by BE97. Namely, if evaporation of stratiform precipitation is instrumental in the formation of the mesoscale vortex, then moister midtroposphere would lead to the formation of a weaker vortex. Even though the presence of a large-scale vortex may have a negative effect via increased inertial stability, it is well known that tropical cyclogenesis and positive large-scale vorticity are correlated (Gray 1968). Perhaps the association of both with convection is a key to their correlation.

As discussed in the introduction, Lunney (1988) found that the ratio of the number of convective elements within the inner 2° of the center to that within 4° of the center was 0.46 in developing cases and only 0.24 in nondeveloping cases. Among our experiments, only the experiment with reduced initial humidity in the midtroposphere did not develop within the first 300 h of simulation time. Figure 13 shows the mean mixing ratio of rainwater within the inner 100 km and from 100 to

300 km from the center. The ratio of outer to inner convection is significantly higher in this experiment than in experiments ST, TR, STNE, and TRNE. This is qualitatively consistent with Lunney's result of outer convection being more dominating in nondeveloping than developing cases.

In the model, downdrafts due to evaporation of precipitation in the inner region are associated with enhancement of peripheral convection. Downdrafts were mitigated in experiments STNE and TRNE by setting evaporational cooling to zero. In reality, any moistening of the inner region of the developing mesoscale vortex may weaken the downdrafts. In BE97, moistening was shown to have occurred in the mesoscale vortex that developed into Hurricane Guillermo, which was an object of intense observations during Tropical Experiment in Mexico (1991). Model simulations showed that moistening could be the result of evaporation of stratiform precipitation in the initial mesoscale convective system (MCS), in which the mesoscale vortex formed. Although the sounding resembled an onion-type sounding (Zipser 1977) during the first hours after the start of the stratiform precipitation in the model, later a moist cold core extended from the midtroposphere into the boundary layer. With sufficient moistening occurring while the vortex forms (in our experiments 90% relative humidity is needed), intensification may occur soon after the formation of the mesoscale vortex. However, Lunney's result suggests that in practice the dominating outer convection plays a role in individual cases of tropical cyclogenesis. Perhaps the moistening while the mesoscale vortex forms is not always sufficient to prevent the occurrence of strong downdrafts that suppress convection in the inner region. More data would be needed from MCSs over the tropical oceans to determine the degree of moistening of vortices that form in them.

6. Conclusions

Simulations with the axisymmetric model showed that intensification of a warm-core, mesoscale vortex occurs as rapidly with a value of the Coriolis parameter from 10° of latitude as with a value from 30° of latitude if the effect of evaporation of precipitation on the temperature is neglected. When evaporation of precipitation is allowed to affect temperature, the onset of rapid intensification occurs after about 70 h of simulation time with the smaller value of the Coriolis parameter and after 150 h of simulation time with the larger value of the Coriolis parameter.

When evaporation of precipitation is fully accounted for in the simulations, it leads to strong downdrafts and weakening of the inner convection near the radius of maximum wind. Meanwhile the outer convection is sustained although its location changes due to downdrafts. This happens both at high and low latitudes. However, important differences are found in the thermodynamic fields between the experiments ST and TR at around 50 h of simulation time, before the rapid intensification in simulation TR takes place. In experiment ST, the boundary layer tangential wind is smaller inside and larger outside the radius of 105 km than in TR (with the exception of the inner 25 km). Moreover, the troposphere is warmer in ST than in TR, and this difference is largest within the inner 120 km.

We suggest that the larger tangential wind speed outside the radius of 105 km at a higher latitude is related to outer convection in an environment with larger inertial stability, or stated differently, conservation of angular momentum in an environment with larger increase of angular momentum with radius. This is supported by Shapiro and Willoughby's (1982) results. They showed that increasing inertial stability in the outer vortex resulted in the most rapid increase of tangential velocity to be larger and closer to the imposed heat source fixed at twice the radius of maximum wind. The differences in the wind and temperature lead to weaker inner convection and stronger outer convection in ST as compared to TR.

To clarify the outer convection's effect on the intensification, we conducted a simulation in which the sea surface fluxes of heat were prevented outside the radius of 184 km. Although this is not an optimal way to test the role of the outer convection because it also affects the inner convection due to advection of drier air, which was demonstrated in Fig. 10, the intensification was shown to occur a little earlier in the experiment with artificially diminished outer convection. This confirms the negative effect of the outer convection for the intensification of the weak mesoscale vortex in the model.

The fact that outer convection may cause spindown of the maximum wind has been shown earlier (e.g., Shapiro and Willoughby 1982; and Montgomery and Enagonio 1998). This is a *direct* effect of outer convection on the intensification of the vortex. In our experiments, however, the spindown of the maximum wind does not occur, presumably due to the presence of *some* inner convection most of the time even before the onset of rapid intensification. Our results suggest that the negative effect of outer convection on the intensification of the vortex may be largely via its *indirect* effect on the location of future convection. Namely, comparison of experiment ST and the same with artificially reduced sea surface fluxes in the outer region (experiment STSSF) showed that the differences in the mass and wind fields between these experiments are consistent with the assumed balanced response to the outer convection, discussed in section 3. This response is unfavorable for the occurrence of inner convection. Especially with the higher value of the Coriolis parameter, the inner convection remains weak for a long time, which slows down the moistening of the inner region. As the onset of rapid intensification in the model only occurs when the inner region has a relative humidity of about 90%, the weak inner convection delays the onset of the rapid intensification of the vortex.

Numerical models that do not include convection as a process that responds to stability may severely underestimate the negative effect of peripheral convection. This is supported by our results that suggest that peripheral convection weakens inner convection by causing changes in the stability of the inner region. As this study suggests that the peripheral convection has a potential to severely delay the onset of rapid intensification of a vortex, we stress that, in nature, there may be factors enhancing the occurrence of the peripheral convection that are absent in our simple simulations.

Use of an axisymmetric model restricts the applicability of the results from the current study. Although simulations of Montgomery and Enagonio (1998) show that the axisymmetrization of initially asymmetric PV anomalies due to peripheral convection occurs efficiently, a three-dimensional model with explicit convection should be used to learn about the net effect of the asymmetric outer convection on the intensification of the vortex.

A goal of future research is to determine the radius outside of which convection delays the start of rapid intensification significantly. The nondimensionalization of Emanual (1989) predicts that the radius depends on the size of the vortex and the value of the Coriolis parameter. As diagnostic methods lack the feedback of the balanced response to convection on the location and strength of future convection, a prognostic model should be used.

Acknowledgments. The author would like to thank Rich Rotunno for his help with using the Rotunno–Emanuel model and Kerry Emanuel and Rich Rotunno for their comments on this paper. The suggestions by two anonymous reviewers significantly improved the paper. Many of the figures were produced using GrADS, originally developed by Brian Doty of COLA. This research was partly supported by the Academy of Finland.

REFERENCES

Bister, M., 1997: Effect of the Coriolis parameter on tropical cyclogenesis: The dominant role of outer convection. Preprints, *22d Conf. on Hurricanes and Tropical Meteorology*, Fort Collins, CO, Amer. Meteor. Soc., 553–554.

——, and K. A. Emanuel, 1997: The genesis of Hurricane Guillermo: TEXMEX analyses and a modeling study. *Mon. Wea. Rev.,* **125,** 2662–2682.

——, and ——, 1998: Dissipative heating and hurricane intensity. *Meteor. Atmos. Phys.*, **50,** 233–240.

Bretherton, C. S., and P. K. Smolarkiewicz, 1989: Gravity waves, compensating subsidence and detrainment around cumulus clouds. *J. Atmos. Sci.*, **46,** 740–759.

DeMaria, M., and J. D. Pickle, 1988: A simplified system of equations for simulation of tropical cyclones. *J. Atmos. Sci.,* **45,** 1542–1554.

Eliassen, A., 1951: Slow thermally or frictionally controlled meridional circulation in a circular vortex. *Astrophys. Norv.,* **5,** 19–60.

Emanuel, K. A., 1986: An air–sea interaction theory for tropical cyclones. Part I: Steady-state maintenance. *J. Atmos. Sci.,* **43,** 585–604.

——, 1989: The finite-amplitude nature of tropical cyclogenesis. *J. Atmos. Sci.,* **46,** 3431–3456.

——, 1994: *Atmospheric Convection.* Oxford University Press, 580 pp.

——, 1995: The behavior of the simple hurricane model using a convective scheme based on subcloud-layer entropy equilibrium. *J. Atmos. Sci.,* **52,** 3960–3968.

——, and R. Rotunno, 1989: Polar lows as arctic hurricanes. *Tellus,* **41A,** 1–17.

Gray, W. M., 1968: Global view of the origin of tropical disturbances and storms. *Mon. Wea. Rev.,* **96,** 669–700.

Khain, A. P., 1984: Modeling tropical cyclone development at different latitudes. *Sov. Meteor. Hydrol.,* **3,** 29–32.

Lunney, P. A., 1988: Environmental and convective influences on tropical cyclone development vs. non-development. Dept. of Atmospheric Science Paper 436, Colorado State University. 105 pp. [Available from Dept. of Atmospheric Science, Colorado State University, Fort Collins, CO 80523.]

McBride, J. L., and R. Zehr, 1981: Observation analysis of tropical cyclone formation. Part II: Comparison of non-developing versus developing systems. *J. Atmos. Sci.,* **38,** 1132–1151.

Möller, J. D., and M. T. Montgomery, 1999: Vortex Rossby waves and hurricane intensification in a barotropic model. *J. Atmos. Sci.,* **56,** 1674–1687.

Montgomery, M. T., and J. Enagonio, 1998: Tropical cyclogenesis via convectively forced vortex Rossby waves in a three-dimensional quasigeostrophic model. *J. Atmos. Sci.,* **55,** 3176–3207.

Ooyama, K., 1969: Numerical simulation of the life cycle of tropical cyclones. *J. Atmos. Sci.,* **26,** 3–40.

Ritchie, E. A., and G. J. Holland, 1997: Scale interactions during the formation of Typhoon Irving. *Mon. Wea. Rev.,* **125,** 1377–1396.

Rosenthal, S. L., 1971: A circularly symmetric primitive equation model of tropical cyclones and its response to artificial enhancement of heating functions. *Mon. Wea. Rev.,* **99,** 414–426.

Rotunno, R., and K. A. Emanuel, 1987: An air–sea interaction theory for tropical cyclones. Part II: Evolutionary study using a nonhydrostatic axisymmetric numerical model. *J. Atmos. Sci.,* **44,** 542–561.

Schubert, W. H., and J. J. Hack, 1982: Inertial stability and tropical cyclone development. *J. Atmos. Sci.,* **39,** 1687–1697.

Shapiro, L. J., and H. E. Willoughby, 1982: The response of balanced hurricanes to local sources of heat and momentum. *J. Atmos. Sci.,* **39,** 378–394.

Simpson, J., E. Ritchie, G. J. Holland, J. Halverson, and S. Stewart, 1997: Mesoscale interactions in tropical cyclone genesis. *Mon. Wea. Rev.,* **125,** 2643–2661.

Sundqvist, H., 1970: Numerical simulation of the development of tropical cyclones with a ten-level model. Part II. *Tellus,* **22,** 504–510.

Wang, Y., and G. J. Holland, 1995: On the interaction of tropical-cyclone-scale vortices. IV: Baroclinic vortices. *Quart. J. Roy. Meteor. Soc.,* **121,** 95–126.

Zipser, E. J., 1977: Mesoscale and convective-scale downdrafts as distinct components of squall-line structure. *Mon. Wea. Rev.,* **105,** 1568–1589.